Science Arena Publications
Specialty Journal of Mining and Geological Engineering
Available online at www.sciarena.com
2018, Vol 1 (1): 11-22

Using Spectral Angle Method to Detect Alterations in Sheets of Mokhtaran and Sarchahshur

Z. Khajehmiri[1]*, M. R. Shayestehfar[2], H. Moeinzadeh[3]

[1] Geological Department, College of Science, University of Kerman, Kerman, Iran,
[2] Department of Mining Engineering, Shahid Bahonar University, Kerman, Iran,
[3] Geology Department, Shahid Bahonar University of Kerman, Kerman, Iran.

***Corresponding Author**

Abstract: *Remote sensing has great importance in exploring mineral deposits especially in arid and semi-arid areas. Identifying altered rocks through remote sensing has been successfully used for the exploration of mineral deposits, especially porphyry copper and gold. In this study, spectral angle method and false color composite were used for processing the ASTER and Landsat images. To detect iron oxides, Landsat 8 images were used, and to detect the minerals such as sericitic, kaolinite, chlorite and epidote. ASTER images were used. In this study, Kaolinite mineral was used for argillic alteration, chlorite and epidote minerals were used for propylitic alteration, sericitic and quartz minerals were used for phyllic alteration, and several areas were selected based on detected alterations. Previous studies in the areas 2, 3, and 4 (in northern parts) introduced this region as epithermal and porphyry systems. The areas 6, 5, 1, were selected for field studies. The area 5 and 1 has the alteration and geology similar to areas 2, 4, and 3. The results of the analysis of mineralized samples taken from areas 5 and 6 showed that these areas have anomaly for the copper, but the area 6 similar to areas 2, 3, 4, and 5 in terms of geology and alteration. Therefore, areas 5 and 6 are recommended for exploration operation.*

Keywords: Spectral Angle, False Color Composite, Mokhtaran, Sarchahshur

INTRODUCTION

Remote sensing is knowledge through which valuable information can be obtained by observing and measuring of an object or land phenomenon from distance and without physical contact with it. In the next stage, useful information can be extracted by analyzing them. Nowadays, remote sensing technique is used widely in world. Remote sensing has great importance in the exploration of mineral deposits, particularly in dry and semi-dry areas. Alteration zones have been widely considered due to being associated with metal reserves and the appropriate characteristics for remote sensing studies. Identification of altered rocks plays critical role in the exploration of epithermal gold and porphyry copper deposits (Amer et al., 2010; Azizi et al., 2010; Di Tommaso and Rubinstein, 2007; Gabr et al., 2010; Sabins, 1997; Pour and Hashim, 2011). Previous studies in this area involved a number of porphyry copper - gold deposits of Shadan and Maherabad, (Malekzadeh Shafaroudi et al., 2014) Khudic epithermal gold (Samiee et al., 2011) and Chahzaghu gold (Shahabi et al., 2005). Due to susceptibility of this region in terms of gold and copper potential, the aim of this research is to identify and introduce other parts of the region that would have alteration and geology similar to the above-mentioned areas. For this purpose, ASTER and Landsat 8 images were used. ASTER has bands which is able to detect the spectral waves at three spectral invisible near infrared (VNIR), short wave infrared

(SWIR), and thermal infrared (TIR) ranges. Three bands are in the visible and infrared range with resolution of 15 meters and 6 bands are in the SWIR range with a resolution of 30 meters, and 5 bands are in the thermal infrared range with a resolution of 90 meters (Abrams, 2000; Yamaguchi et al., 1999). Six bands of SWIR have the capability to detect AL-OH, Fe Mg-OH.CO3. Studies have shown that hydrothermal alteration and minerals of alunite, kaolinite, chlorite, talc, calcite, and dolomite can be detected in the SWIR band (Crosta et al., 2003; Diommaso and Rubinstein, 2007; Ducart et al., 2006; Rowan et al., 2005). Iron oxides (hematite, goethite, and limonite) have spectral absorption characteristics in the visible near infrared (VNIR) range (Boloki and Poormirzaee, 2009). In this study, this spectral range was used for detecting of iron oxides that due to the high number of bands in this waves range in the Landsat 8 sensor compared to ASTER for the detection of iron oxides, Landsat 8 was used. Landsat 8 was laced on Earth's orbit in February 2013. Landsat 8 has 11 bands in the wavelength of visible, near infrared, short infrared, thermal infrared and short infrared short. It has also spatial resolution of 30 m for the range of visible, near infrared, short infrared, and the spatial resolution of 100 m for thermal infrared and one panchromatic band with resolution of 100 m. Having 5 bands in the range of the visible and near-infrared provides appropriate data for the detection of iron oxide. (Ben-Dor et al., 1994; Scheidt et al., 2008)

The geographical location of the studied area:

The studies area included a frame with dimensions of 60 x 60 km that its specifications are shown in Table 1. This area contains 1: 100,000 geological sheets of Mokhtaran and Sarchahshur and major part of it are in the 100000 sheet of Mokhratan. In terms of geographical location, this area is located in South Khorasan province in East Iran, and its geographical location in the WGS84 system is in the 59 º 24’ 10”- 58 º 43’ 42” longitude, and 32 º 00’ 00” -32º 10’ 00” latitude. Figure 1 shows the geographical location of the studied area in the South Khorasan province of Iran.

Geology of the studied area:

In the structural divisions of Iran, the eastern part of the studied area is located in the western edge of the flysch or colored mélanges of the Zabol-Baloch zone and its western parts is located in the Lut block. The Zabol-Baloch zone is located in the west and Helmand is located in the east. Flysch zone has been tectonized and deformed. This zone comprises deposits such as siliceous shales, radiolarites and pelagic limestones and volcanic rocks such as basalt, split basalts, diabase, dacite, rhyolite, and serpentinized ultrabasic rocks. In general, rocks of this zone are divided into several categories, including 1- flysch deposits 2- volcanic rocks and intrusive rocks, and 3. Ophiolite units (Aghanabati, 2004). Lut block has 900 km length, which its northern border is Daruneh fault in South of the Jazmvzyan troughs and its western bourder is camel, and east of it is Taybndan fault.

Most parts of the studied area are located in the Lut block. Lut block contains large volumes of volcanic and sub-volcanic rocks. Lut block is one of the sub-continents separated from the northern margin of Gondwana and attached to Eurasia during the early Triassic age. It coincides with closing of Paleotethys. Volcanic and sub-volcanic rocks with thickness of 2000 m cover the Lut block (Berberian et al., 1999; Camp, Griffis, 1982; Tirrul et al., 1983) and they were formed during subduction and collision of the Arabic and Asian age. Types of mineralization in this block are related to to subduction under the Lut block in Tertiary such as mineralization type IOCG in Ghale Zari (Geol et al., 2005; Richards et al., 2012), copper – gold type porphyry in Maherabad (Pour and Hashim, 2011), copper in Sheikh Abad and Hamych (Karimpour et al., 2007; Arjmandzadeh et al., 2011) Copper type porphyry in Dehsalm (Arjmandzadeh et al., 2011), Kuhesorkh (Abdi et al., 2010), Khonik gold (Malekzadeh Shafaroudi et al., 2014; Malekzadeh et al., 2010), Hired gold (Karimpour et al., 2007). The geological sheet 1: 100,000 in Mokhtaran include medium igneous rocks to acidic andesite, dacite, Rhyodacite with Tertiary age and colored melange with upper Cretaceous age. Clear boundaries are seen from listwaenitic in vicinity of ultrabasics and basic rocks, and its southern part includes gneiss plagioclase lenses biotite-rich granite. In addition, a circular collection of granite to sub-volcanic micro-granodiorites is seen inside the andesite and tuff Paleogene on this map.

Clay geological sheet 1: 100,000 in Chahshur includes relatively folded Tertiary volcanic zones of Kuh-Shah in north (continuation of volcanic units of sheet 1,000,000 of Mokhtaran), relatively altered Cretaceous flysch and the collection of colored melange stretched from North West to the South East. Types of basics ranging from basaltic andesites and anhydrites cut by diorite dikes are seen in the south west of the map. In geological map (Figure 2), rock units placed within the studied area are displayed briefly and adapted from 1: 100000 geological map of Mokhtaran and Sarchahshur.

Materials and Methods

Before using the data, they should be prepared for the stage of processing. Preprocessing operation to prepare data for the studies area included:

A. Geometrically correction using image-to-image and atmospheric correction (IARR) considered on the studied area
B. Determining ASTER bands and applying false color composite (FCC) techniques
C. Spectral Angle Mapper (SAM)
D. Preparation of alteration map of studied area
E. Conducting the field visit stage and sampling from detected areas during satellite data processing in the studied area,

Preparation of false color map

In this method, by putting right bonds of image in the red, green and blue boxes, the desired outcomes emerge in the desired colors in image so that desired outcomes to be extracted easily from the image. In this study, to understand the area and its alterations, false color composite map (RGB) was used firstly. Then, for accurately separation of the alteration areas, spectral angle was used. Experimental analyzes have shown that in the ASTER images, the image with composite of RGB=468 is the most appropriate color composite to detect the alteration in most of the deposits, especially porphyry copper and epithermal gold (Tommaso and Rubinstein, 2007; Kruse et al., 1993) and the obtained image is shown in Figure 3 for the considered area based on this color composite. In this image, areas with propylitic alteration are seen in green color, and areas with kaolinite, alunite and sericitic alteration are seen with pink color. This is due to high reflectivity of alunite, and kaolinite and muscovite minerals in band 4 compared to bands 6 and 8. To detect kaolinite, sericitic, chlorite, epidote, quartz, hematite, jarosite, spectral angle method and ASTER images alterations were used, and to detect the iron oxides (hematite - jarosite), satellite images of Landsat 8 were used.

Spectral angle method

Spectral angle mapper method was used for the first time in 1993 by Kruse et al. This method is based on the similarity between a reference mineral and tested mineral test spectrum and the Pixel spectrum is evaluated by calculating the angle between spectra (spectra are considered in the form of vectors in a multi-dimensional space in which space dimensions depend on the number of bands). The angle between reflecting spectrum and the reflected spectrum from the surface of pixels is considered as the similarity criterion.

This technique will be different in terms of albedo and lightning effects and it is not affected by solar lighting factors, since the angle between two vectors is independent of their lengths. In the image obtained from the spectral angle mapper method, each pixel represents the reflection difference in the resolution spectra of the reflected spectral model from its surface with reference spectral model. In the output of spectral angle mapper, the brighter pixel is equivalent to larger angle, and it represents higher difference of the studied spectrum with the reference spectrum and darker pixel is equivalent to smaller angle and sign of greater similarity of the spectra (Van der Meer, De Jong, 2003). In this study, ASTER data were processed and determined after topography and geometric correction and integration of SWIR and VNIR bands to detect the various minerals of alteration zones index. For processing using spectral angle mapper (SAM) in the considered area, 40 spectra were extracted and the spectra extracted from the area were compared with library spectra USGS. min. sil. Then, type of mineral of extracted spectra of the area was determined based its comparison with library extracted spectra (Table2). Finally, using this determined spectrum and using spectral angle, argillic (Kaolinite), phyllic (sericitic, silica), propylitic (epidote, chlorite) and iron oxides (Hematite and jarosite) alterations were detected (Figures 4a-4d).

Discussion and Results

In Figure 5, areas have been determined in terms of alterations. The specification of some of these areas as follows:

Area No 2: this area has argillic, phyllic, silica, jarosite and Hematite alterations. This area has been introduced based on previous work as an epithermal epithermal gold (Khunik gold) (Malekzadeh Shafaroudi et al., 2014).

Areas 3 and 4: these areas have argillic, phyllic, jarosite and silica, hematite, alterations based on previous works. This area have been introduced as a system of porphyry copper and gold (The area of Maher Abad - Shadan) (Arjmandzadeh et al., 2011; Abdi et al., 2010).

Area No 5: this area is located in the North of the studied region, including argillic, phyllic, silica, jarosite and Hematite alterations. In terms of geology, based on the geological map 1:100000, it includes dacite, andesite, and altered tuffs that granite and diorite masses have been penetrated in some parts. A number of sample was taken of this area to investigate the petrography and mineralization studies. The results of analysis of mineralized samples are shown in Table 3. In this table, the rate of copper is 6% in the sample No KBP16, and the images of alterations observed in this area have been determined in Figures 6 a-d. In figures 7-a and b iron-bearing minerals have cut the quartz veins.

Area No. 6: this area has the silica, propylitic (chlorite, epidote), Hematite and a little argillic (kaolinite) alterations and the geology of this area based on the geological map 1: 100000 includes listwaenitic, flysch, and diabase rocks that silica is in the form of is a form of field visits in listvenite veins in flied visits. These alterations have been determined in Figure 8. It noteworthy that according to Table 4, the element of copper has been shown in this area anomaly. According to alteration and host rocks observed, the type of this mineralization varies with areas of 3 and 4 in this area, which requires further investigation.

Area No 7: it has Propylitic, hematite, silica and a small amount of argillic alterations. The rock units in this area include ultrabasic, listwaenitic, shale, and sandstone rocks.

The area No 8 has hematite, silica, propylitic, and small amount of Kaolinite that based on previous studies is copper-gold (Shahabi et al., 2005).

Conclusion

Using ASTER and Landsat 8 image in the studies area (located in sheet 1: 100000 of Mokhtaran and Sarchahshur) and applying the spectral angle method on the detected alterations in the area include sericitic, silica (phyllic alteration) and kaolinite (argillic alteration), jarosite, Hematite, and propylitic (epidote and chlorite). In the northern and Western parts of the studied area, the host area of these alterations is the dacitic, andesite rocks and generally acidic volcanic rocks at the moderate level. In the eastern parts, the studies area of the host rocks included ultrabasic and diabase rocks and the intensity and type and rate of alteration vary in them. In the alteration map prepared from the studied region, the areas 2, 3, and 4 based on previous studies conducted, the mineralization of the copper is type of porphyry and epithermal. Finally, considering the similarity of District 5 and 1 alterations and lithology with areas 3, 4, and 2 and according to the results of in the area 5, it is recommended that exploration operation to be conducted in these regions. The area No 6 also requires exploration operation according to analyses. It noteworthy that type of alteration and lithology in the area 6 with areas 2, 3, 4, and 5 varies.

References

1. Abdi, M., Karimpour, M.H. and Najafi, A., (2010). Geology, alteration and mineralizationpotential of Kuh-Shah region. South Khorasan. First Symposium of IranianSociety of Economic Geology, Mashhad, Iran, pp. 1–7.
2. Abrams, M. (2000). The advanced spaceborne thermal emission and reflection radiometer (ASTER): data products for the high spatial resolution imager on NASA's Terra platform. Int. J. Remote Sens. 21, 847–859.
3. Aghanabati.(2004) . Geology of Iran, publish of geology survey of Iran (in Persian).
4. Amer, R., Kusky, T.and Ghulam, A. (2010). Lithological mapping in the central eastern desert of Egypt using ASTER data J. Afr. Earth Sci. 56, 75–82.
5. Arjmandzadeh, R. Karimpour, M.H. Mazaheri, S.A. Santos, J.F. Medina, J.M. Homam, S.M. (2011). Sr–Nd isotope geochemistry and petrogenesis of the ChahShaljami granitoids (Lut Block, eastern Iran). J. Asian Earth Sci. 41, 283–296.
6. Azizi, H., Tarverdi, M.A. and Akbarpour, A. (2010). "Extraction of hydrothermal alterations form ASTER SWIR data from east Zanjan, northern Iran". Adv. Space Res. 46, 99–109.
7. Ben-Dor, E., Kruse, F.A. ,Lefkoff, A.B. and Banin, A. Comparison. (1994). three calibration techniques for utilization of GER 63-channelaircraft scanner data of Makhtesh Ramon, Nega, Israel, Photogramm. Eng. Remote Sens. 60 (1339–1354).
8. Berberian, M., Jackson, J.A., Qorashi, M., Khatib, M., Priestley, K., Talebian, M. and Ghafuri-Ashtiani, M.(1999). Faulting along the Sistan suture zone of eastern Iran. Geophys. J. Int. 136, 671–694.
9. Boloki, M. and Poormirzaee, R.(2009). Using ASTER Image Processing for Hydrothermal Alteration and Key Alteration Minerals Mapping in Siyahrud area, Iran. International Journal of Geology, 3: 38-43.
10. Camp, V. Griffis, R. (1982). Character, genesis and tectonic setting of igneous rocks in the Sistan suture zone,
11. Crosta, A.P., Souza Filho, C.R., Azevedo, F. and Brodie, C.(2003).Targeting key alteration minerals in epithermal deposits in Patagonia, Argentina, using ASTER imagery and principal component analysis. Int. J. Remote Sens. 24, 4233–4240.
12. Di Tommaso, I.and Rubinstein, N. (2007). Hydrothermal alteration mapping using ASTER data in the Infiernillo porphyry deposit, Argentina. Ore. Geo.Rev. 32, 275–290.
13. Diommaso, I. and Rubinstein, N. (2007). Hydrothermal alteration mapping using ASTER data in the Infiernillo porphyry deposit, Argentina. Ore. Geo.Rev. 32, 275–290.
14. Ducart, D.F., Crosta, A.P. and Filio, C.R.S. (2006).Alteration mineralogy at the Cerro La Mina epithermal prospect, Patagonia, Argentina: field mapping, short-wave infrared spectroscopy, and ASTER images.Econ. Geo. 101, 981–996.
15. Gabr, S, Ghulam. and A. Kusky, T. (2010).Detecting areas of high-potential gold mineralization using ASTER data. Ore Geo. Rev. 38, 59–69.
16. Geol. Soc. Am. Bu Karimpour, M.H. Larg, R.R. Razmara, M. Pattrick, R.A.D.(2005). Bi sulfosalt mineral series paragenetic associations in specularite-rich Cu–Ag–Au deposit, QalehZari mine, Iran. Iran. Soc. Crystallogr. Mineral. 13 (2), 417–432ll. 94, 134–156.
17. Karimpour, M.H., Malekzadeh Shafaroudi, A., Mazaheri, S.A.,& Haidarian Shahri, M.H.(2007).Magmatism and different types of mineralization in Lut Block. In: 15th Symposium of Iranian Society of Crystallography and Mineralogy, Ferdowsi University of Mashhad, Iran.
18. Kruse, F. A. Lefkoff, A. B. Boardman ,J. B. Heidebrecht, K. B. Shapiro, A. T. Barloon P. J. Goetz, A. F. H. (1993). The Spectral Image ProcessingSystem (SIPS) - Interactive Visualization and Analysis of

Imaging Spectrometer Data, RemoteSensing of Environment, Special issue on AVIRIS, v. 44 , 145 - 163.

19. Malekzadeh Shafaroudi, A., Karimpour, M.H . and Stern, C.R.(2014) The Khopik porphyry copper prospect, Lut Block, Eastern Iran: geology, alteration and mineralization,m fluid inclusion, and oxygen isotope studies. Ore Geol. Rev.
20. Malekzadeh, A., Karimpour, M.H.and Mazaheri, S.A. (2010). Rb–Sr and Sm–Nd isotopic compositions and Petrogenesis of ore-related intrusive rocks of gold-rich porphyry copper Maherabad prospect area (north of Hanich), east of Iran. J.Crystallogr. Mineral. 18, 15–32.
21. Pour, B.A. and Hashim, M. (2011). Identification of hydrothermal alteration minerals for exploring of porphyry copper deposit using ASTER data, SE Iran J. Asian Earth Sci. 42, 1309–1323.
22. Richards, J.P., Spell, T., Rameh, E., Razique, A., Fletcher, T. (2012). High Sr/Y magmas reflect arc maturity, high magmatic water content, and porphyry Cu ± Mo ± Au potential: examples from the Tethyan arcs of central and eastern Iran and western Pakistan. Econ. Geol. 107, 295–332.
23. Rowan, L.C., Mars, J.C.and Simpson, C.J. (2005).Lithologic mapping of the Mordor N.T, Anstralia ultramafic complex by using the advanced spaceborne thermal emission and reflection radiometer (ASTER).Remote Sens. Environ. 99, 105–126.
24. Sabins, F.(1997). Remote Sensing Strategies for Mineral Exploration, in: Rencz, A.E. (Ed.), Remote Sensing for the Earth Sciences. John Wiley & Sons, Inc., New York, USA, pp. 375–447.
25. Samiee,S.,Karimpour, M.H., Ghaderi, M.and Haidarian Shahri, M.R. (2011). Geology, alteration and mineralization potential in Khonic area, south of Birjand, The second Congress of economic geology of Iran.
26. Scheidt, S. and Ramsey, M. ancaster, N.(2008). Radiometric normalization and image mosaic generation of ASTER thermal infrared data:an application to extensive sand and dune fields, Remote Sens.Environ. 112, 920–933.
27. Shahabi, M.H., Askari,A. and Shahabpour, J.(2005). Geochemistry and economic assessment of Listvenite of chahzaghoo, Fourteenth Congress of Crystallography and Mineralogy of Iran.
28. Tirrul, R., Bell, I.R., Griffis, R.J. and Camp, V.E. (1983). The Sistan suture zone of eastern Iran.
29. Tommaso, D. I. and Rubinstein, N. (2007). Hydrothermal alteration mapping using ASTER data in the Infiernillo porphyry deposit, Argentina.Ore Geology Reviews, 32: 275-290
30. Van der Meer, F. De Jong, S. (2003). ImagingSpectrometery. Basic Principles and Prospective Applications, 4. Kluwer Achademic Publishers,Dordrecht/ Boston/ London.
31. Yamaguchi, Y.I., Fujisada, H., Kudoh, M., Kawakami, T. and et al. (1999). ASTER instrument characterization and operation scnorio. Adv. Space Res. 23 (8), 1415–1424.

Table 1. Specifications of ASTER images of the study area (USGS, 2001)

Date picked up	Image dimensions	Circulation rate	Geographic coordi-nates in the northwest corner	File format	Correction level	File name
6/9/2001	60 * 60 km	7,980704	32,53918333.N 58,67563333 .E	hdf	level 1B	aster1b_090601_322

Table 2. Selected optimal spectral angles for hydrothermal alteration minerals in the study area in spectral angle method

Hematite	Jarosite	Silica	Epidote	Chlorite	Sericite	Kaolinite	Mineral
0.27	0.19	0.008	0.035	0.035	0.032	0.098	spectral angles

Table 3: Results of analysis of samples taken from the anomal No. 5

Sample	Au	As	Bi	Cu	Mo	S	Pb	Zn	Sb
Unit	Ppb	Ppm	Pp	Ppm	Ppm	Ppm	Pp	Ppm	Ppm
KBP16	0.75	4.7	0.43	81	4.19	71	14	37	1.38
KBP161	154	32.6	4.8	68729	21.8	17001	420	342	1.4
KBP162	0.75	26.9	0.56	225	4.4	281	18	12	1.19
KBP163	0.75	8.1	0.26	108	16.24	305	14	13	1.19
KBP164	0.75	113	3.8	22	1.66	964	10	14	1.22

Table 4: Results of analysis of samples taken from the anomal No. 6

Sample	Au	As	Bi	Cu	Mo	S	Pb	Sb
Unit	Ppb	Ppm	Ppm	Ppm	Ppm	Ppm	Ppm	Ppm
KBE1	34	5.3	0.38	108050	0.98	15747	450	0.78
KBE2	18	5.3	0.52	135	1.02	104	23	0.98
KBE3	28	17.5	0.9	22055	14	383	188	0.73
KBE4	13	10.1	0.52	11660	9.96	149	147	0.76
KBE5	19	13.5	0.81	22392	24	1850	148	0.66
KBE6	32	5.2	0.69	947	1.08	117	456	0.69

Figure 1: Geographical location of the studied area in South Khorasan province of Iran

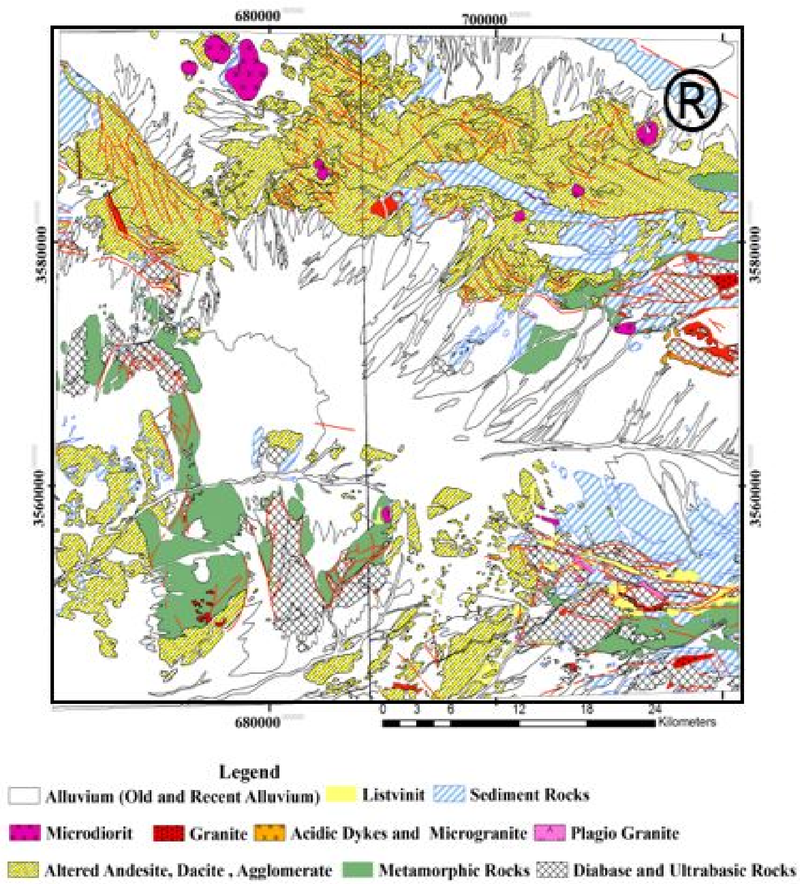

Figure 2: Geology of the studied area adopted from geological maps of Mokhtaran and Sarchahshur

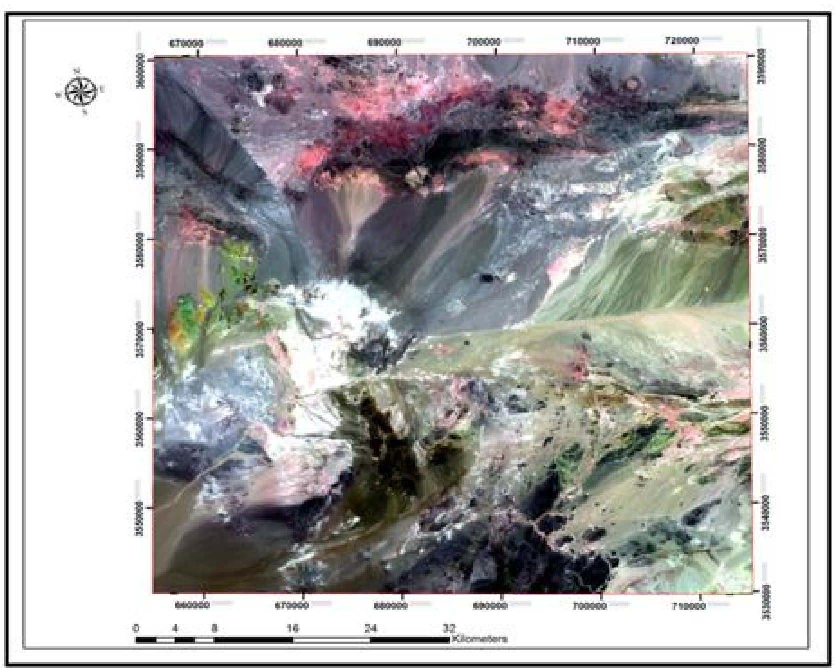

Figure 3: Detection of the alterations using false color composite in the ASTER image RGB=468. In this image, pink color indicates argillic alteration and green color indicates propylitic alteration.

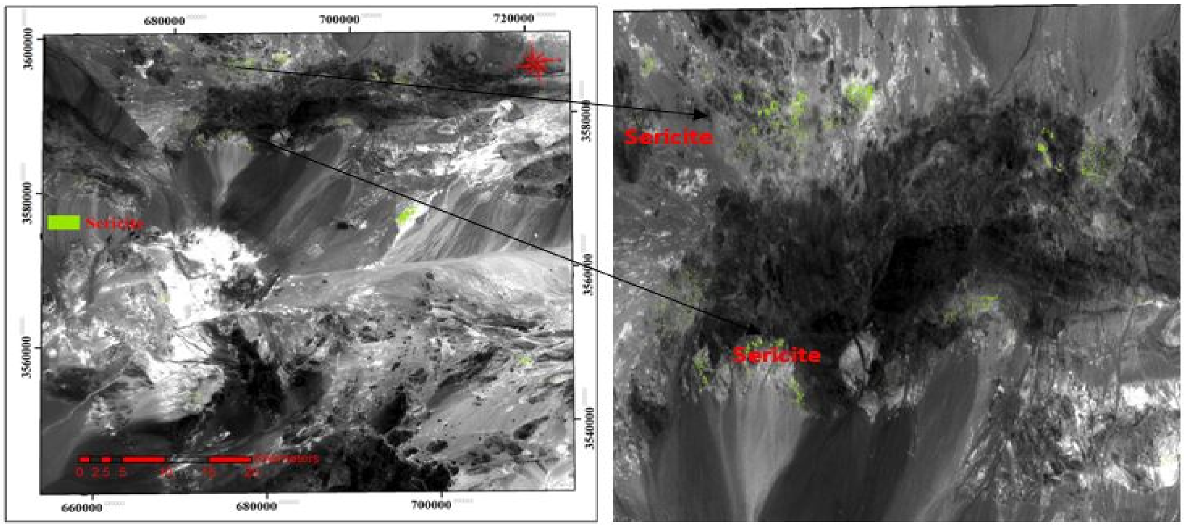

Figure 4 a: detecting sericitic mineral using spectral angle

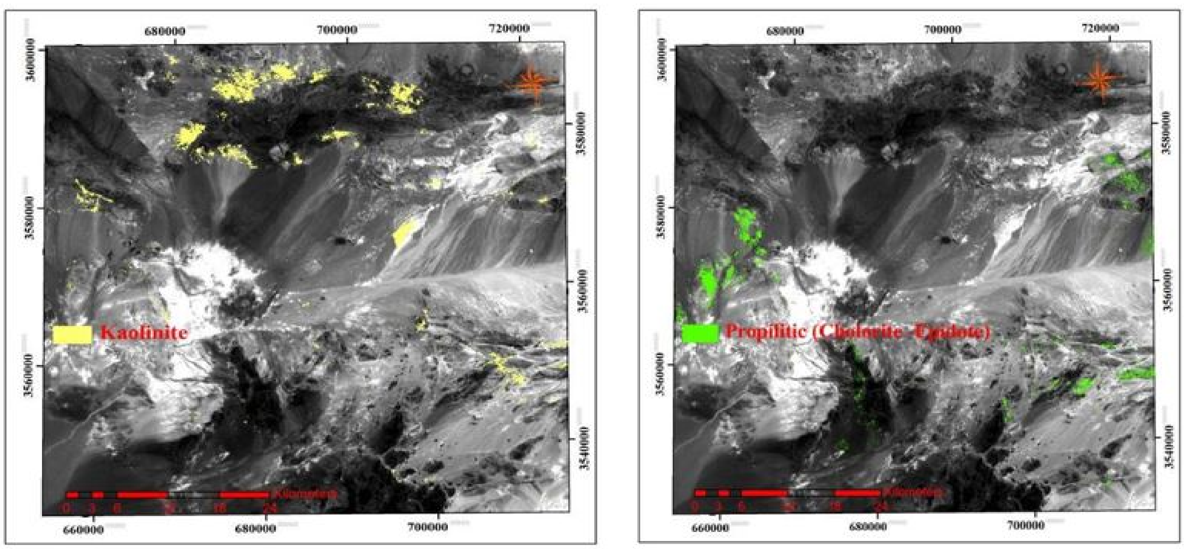

Figure 4 b: detection of Chlorite and epidote and kaolinite minerals using

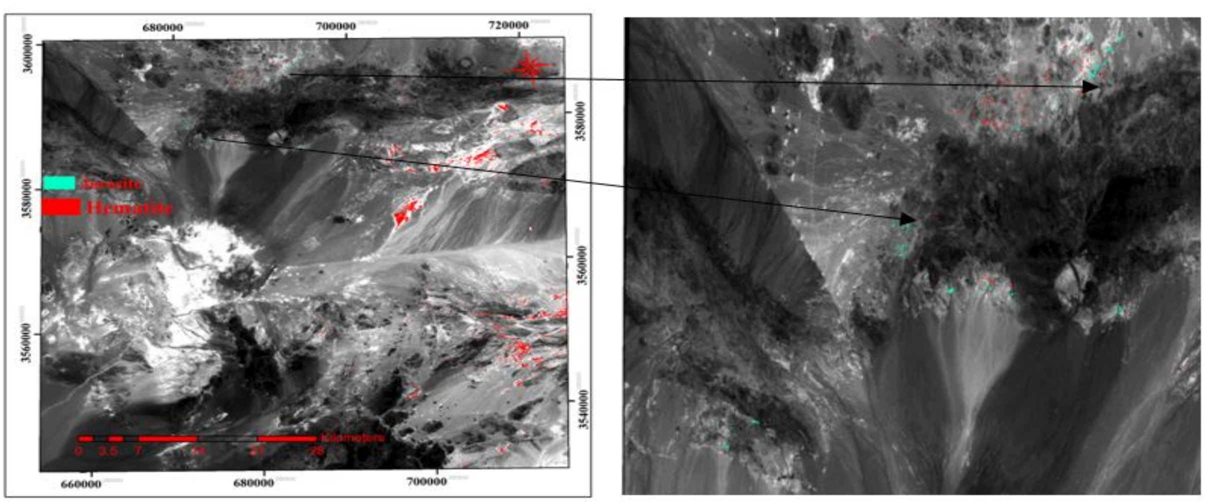

Figure 4 C: detection of hematite and jarosite minerals using spectral angle

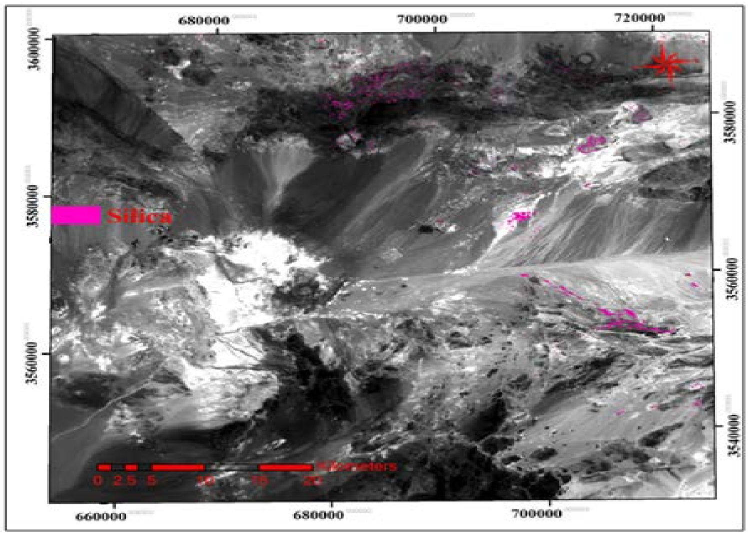

Figure 4 D: detection of silica mineral using spectral angle

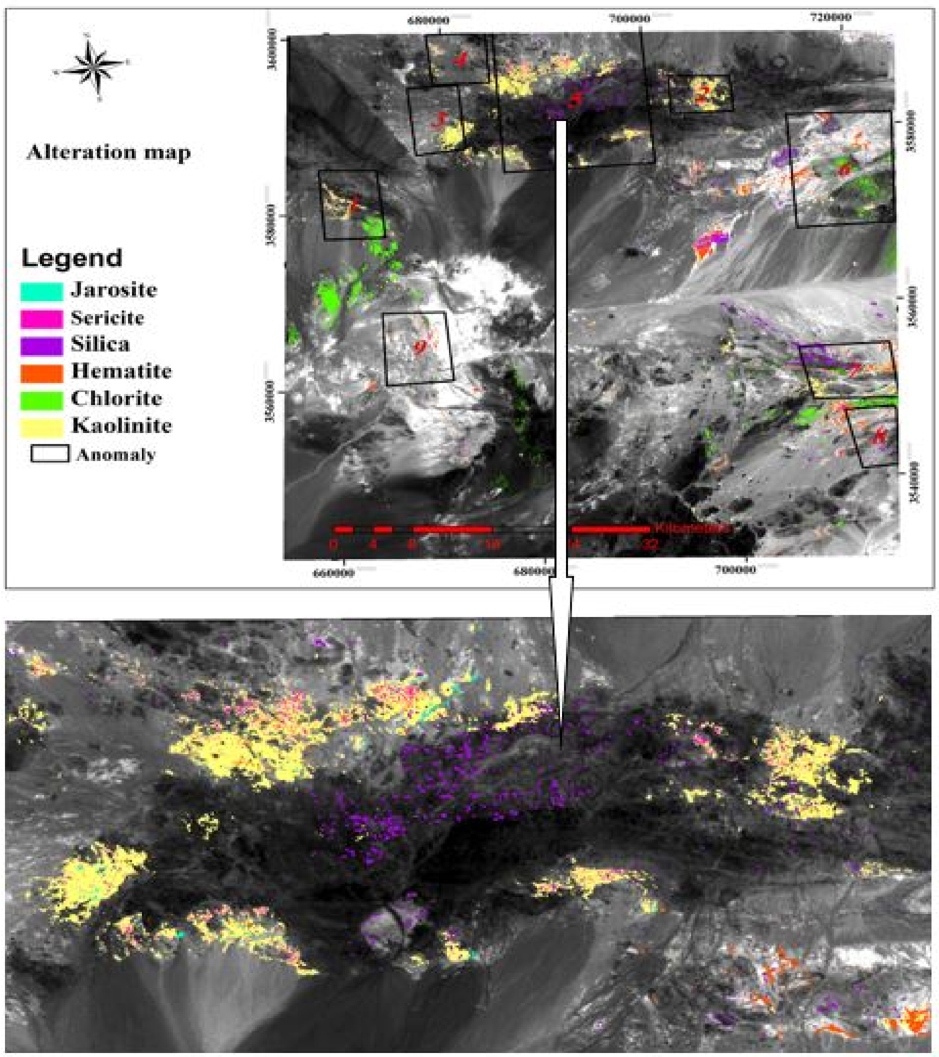

Figure 5: display of alterations studied area and anomaly areas based on alterations

Figures 6 a - d: include a lterations of area (5) (a): siliceous veins, b argillic, c: sericite and argillic.

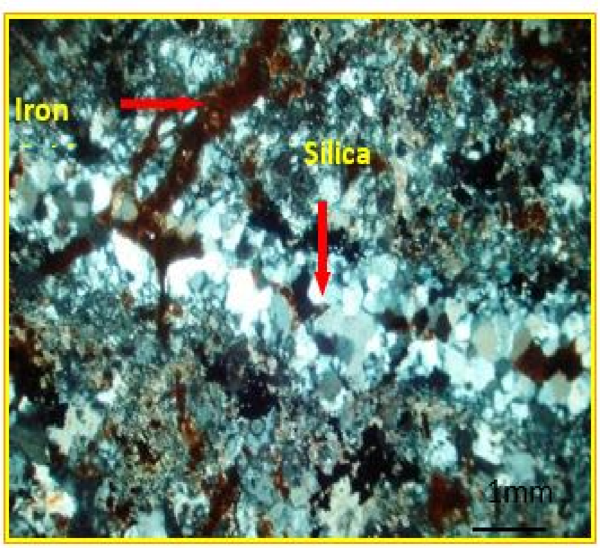

A

B

Figures 7 (a) - (b): silica veins cut by iron veinlets A) in microscopic sample and B) in field sample

Figures 8 (a) - (d): alterations observed in the anomaly area 6: (a) argillic alteration, (b) alteration of iron oxide (c) propylitic alteration, (d) silica alteration